Journal of Zhejiang University SCIENCE A
ISSN 1673-565X (Print); ISSN 1862-1775 (Online)
www.zju.edu.cn/jzus; www.springerlink.com
E-mail: jzus@zju.edu.cn

CFD simulation with enhancement factor of sulfur dioxide absorption in the spray scrubber*

Xiang GAO†, Wang HUO, Zhong-yang LUO, Ke-fa CEN

(*State Key Laboratory of Clean Energy Utilization, Institute for Thermal Power Engineering, Zhejiang University, Hangzhou 310027, China*)

†E-mail: xgao@cmee.zju.edu.cn

Received July 3, 2008; revision accepted Oct. 15, 2008

Abstract: A model describing the absorption process of SO_2 into limestone slurry with a spray scrubber is presented. Both the physical performance of the spray liquid in the scrubber and the involved chemical reactions are analyzed in the model. A continuous concentration change of H^+ was solved by iterative coupling using Matlab, and it was found that there was a remarkable influence on the concentration of the other elements in the process of SO_2 absorption. The calculations show that the enhancement factor exponentially grows with an increasing value of pH and logarithmically decays with an increasing value of the driving force. To verify the accuracy of the model, experiments were also carried out, and the results suggest that the model, after combining the physical performance of the spray and the enhancement factor, can more precisely describe SO_2 absorption in a spray scrubber. Furthermore, a commercial computational fluid dynamics (CFD) tool is used to perform several simulations which describe and clarify the effects of variables on SO_2 absorption. The results of numerical simulation can provide a basis for further design and optimization of the scrubber.

Key words: SO_2 absorption, Limestone dissolution, Enhancement factor, Mass transfer, Concentration profile
doi:10.1631/jzus.A0820507 **Document code:** A **CLC number:** X5; X7

INTRODUCTION

It has been long commonly accepted that, besides being a hazard to the human body, the emission of sulfur dioxide caused by coal-fired power plants pollutes the atmosphere. This can lead to negative environmental impacts such as acidification of soil and global warming (Zhang *et al*., 2007). Many solutions have been employed to desulphurize the exhaust flue gas from power plants, such as spray towers, venturi scrubbers, and static and mobile packed beds. However, countercurrent spray absorbers, using limestone slurry as the absorbent and targeting high volume flue gas desulphurization, are the most recognized method. This is mainly due to the high efficiency of SO_2 removal, the comparatively low cost, the simple process, and the wide availability of the absorbent.

The absorption process of SO_2 in alkaline solution has been studied for decades. There are several key processes involved in desulphurization, such as liquid-gas mass transfer, limestone dissolution, sulfite oxidation, gypsum crystallization, etc. However, the mass transfer between gas phase SO_2 and limestone slurry drops is the key part of the absorption process. Many studies have been done to investigate the effects on SO_2 removal efficiency from the physical and chemical properties of the diffusing gas and the hydrodynamics of the moving alkaline drops (Ebrahimi *et al.*, 2003; Nagel *et al*., 2002; Bausach *et al.*, 2006).

A number of mathematical models have been proposed and many experimental investigations have been carried out in order to provide better understanding of mass transfer from gas into water drops, which was found to be controlled by both the continuous-phase (Altwicker and Lindhjem, 1988; Saboni

* Project supported by the National Key Technologies Supporting Program of China during the 11th Five-Year Plan Period (No. 2006BAA01B04) and the New Century Excellent Talent in University (No. NCET-06-0513), China

and Alexandrova, 2001; Kadja and Bergeles, 2003) and the liquid-phase (Amokrane and Caussade, 1999). Based on the two-reaction model of SO_2 absorption in an alkaline solution, a penetration theory was presented (Hikita *et al*., 1972). The process of SO_2 absorption was simulated and it was concluded that the absorption is largely controlled by the liquid-side (Brogren and Karlsson, 1997). During absorption of SO_2 in a bubbling reactor, the liquid side mass transfer was studied (Lancia *et al*., 1994) and an absorption model with a reaction plane was developed (Sheng and Wen, 2006). Also, close to the nozzle, Yeh and Rochelle (2003) found that approximately 60% of mass transfer occurs in the liquid sheet before droplet formation, and that the droplet region can account for less than half of the total mass transfer. Furthermore, Alexandrova *et al.*(2004) analyzed fractional liquid resistance to mass transfer for falling droplets in various concentrations of SO_2 and showed that the fractional liquid resistance is independent of the droplet diameter.

The absorption of SO_2 in a limestone slurry scrubber is a complex process that contains both mass transfer and a chemical reaction. A better understanding of this complex mass transfer is needed for further optimization of scrubber design. More recently, with the help of computer technology combined with fluid dynamics, computational fluid dynamics (CFD) has been developed and used to study the transport behavior in two or three phase flows (Scala *et al*., 2004; Retieb *et al*., 2007; Kota and Langrish, 2007). CFD models were reported and used for the simulation of the process of WFGD (Wet Flue Gas Desulphurization) plant (Gomez *et al.*, 2007). However, the assumed pH mass transfer coefficient and enhancement factor made these models of limited use in describing the continuous SO_2 absorption process in an absorber. Further improvement can be achieved by considering the physical performance of the spray liquid and the continuous change in H^+ concentration in the process of absorption.

In order to address the absorption process in detail, a model combining the absorber tower and oxidation tank has been presented and solved using Matlab by iteratively coupling the concentration change of H ions. The enhancement factor representing chemical reactions is investigated and an alkaline absorbent ($CaCO_3$) is used to clarify the SO_2 concentration distribution. The performance of the falling drops was simulated by interpolating the enhancement factor into the user defined function (UDF) of CFD. Furthermore, several typical operation parameters in WFGD are selected to clarify their influences on the process of SO_2 absorption.

MODEL

Based on interaction between flue gas and slurry in the absorption process, the model is formulated using the following assumptions:

(1) The flue gas is treated as incompressible flow and the effects of vapor and inner parts of the absorber on the flue rate are omitted;

(2) The droplets are assumed to remain spherical, and breakage and consolidation in the falling process are not considered (Akbar *et al*., 2003);

(3) Because of lower partial pressure of oxygen in the gas phase, sulfite oxidization and gypsum crystallization are assumed to be only achieved in the tank;

(4) The heat of reaction and dissolution is small and can be neglected, and the system is considered to be isothermal;

(5) The wall effect is ignored and the SO_2 absorption is assumed to take place in parallel with the limestone dissolution;

(6) The size distribution of initial drops of limestone slurry obeys the rule of Rosin-Rammler.

Movement of droplets

When the absorbent is injected from the nozzle, the slurry movement can be described by combining the gravity of downside drops with the upside gas drag:

$$h=\int_0^t u_{\mathrm{d}}\mathrm{d}t, \tag{1}$$

$$\frac{\mathrm{d}u_{\mathrm{d}}}{\mathrm{d}t}=g\left(\frac{\rho_{\mathrm{d}}-\rho_{\mathrm{g}}}{\rho_{\mathrm{d}}}\right)-\frac{3}{4}\left[\frac{\rho_{\mathrm{g}}(u_{\mathrm{d}}-u_{\mathrm{g}})^2\zeta_{\mathrm{d}}}{\rho_{\mathrm{d}}}\right], \tag{2}$$

$$\zeta_{\mathrm{d}}=\frac{24}{Re_{\mathrm{d}}}(1+0.19Re_{\mathrm{d}}^{0.65})+\frac{0.44Re_{\mathrm{d}}}{7185+Re_{\mathrm{d}}}, \tag{3}$$

where h is the dropping distance of droplet; u is the velocity and ρ is the density; subscripts 'g' and 'd' denote the flue gas and droplet, respectively; ζ_{d} is the drag coefficient of droplet which can be drawn from the calculation of Haider and Levenspiel (1989).

Calculation of mass transfer coefficient

According to the size distribution of droplets (d), the equation of Rosin-Rammler was adopted:

$$Y_d = e^{-(d/\bar{d})^n} \quad (\bar{d}=94.5\ \mu m;\ n=4.5), \tag{4}$$

$$Sh = \frac{k_g R' T \bar{d}}{D_g P} = 2 + 0.55 Re_d^{0.5} Sc_d^{0.33}, \tag{5}$$

$$Re_d = \frac{\bar{d}(u_d - u_g)\rho_g}{\mu_g}, \tag{6}$$

$$Sc_d = \mu_g / (\rho_g D_g), \tag{7}$$

where $\bar{d}$ is the average diameter of the droplets and k_g is mass transfer coefficient of gas phase which can be obtained by the widely used correlation for spherical droplets (Gerbec *et al*., 1995). D is the diffusion coefficient and the dimensionless Reynolds number for droplets (Re_d) is based on the relative velocity between the droplets and the surrounding gas. The calculation of the Schmidt number of droplets (Sc_d) is based on the physical identity of SO_2. Sh is the dimensionless Sherwood number and μ is the turbulent viscosity.

However, k_L which is mass transfer coefficient of liquid phase, is a more complicated issue in the spray. The effective mass transfer coefficient for the liquid phase is separated into a physical mass transfer coefficient, which accounts for diffusive and convective contributions to mass transfer. In this paper, k_{Ls} and k_{Ld} are used to describe mass transfer coefficients of liquid phase in liquid continuous region and in the spray droplets region, respectively. Close to the nozzle, k_{Ls} is applied to a liquid continuous region and can be calculated by:

$$\frac{k_{Ls} h_0}{2D_L} = C_0 Re_0^{C_1} We_0^{C_2} Sc_0^{0.5} (r_0 / L_0)^{C_3}, \tag{8}$$

where $\ln C_0=-3.8$, $C_1=-1.5$, $C_2=0.7$, $C_3=-2.7$ (Yeh and Rochelle, 2003), and

$$r_0 = d_{or}/2 - h_0 \cos(\theta/2), \tag{9}$$

where r_0 is the distance from the nozzle, θ is the spray angle. L_0 is the sheet breakup length which is decided by the diameter of the orifice of nozzle (d_{or}) and the liquid sheet velocity (U_0). The subscripts 'L' and '0' denote the liquid phase and the liquid sheet, respectively. The parameters can be calculated by using Eqs.(10)~(15):

$$Re_0 = \frac{h_0 U_0 \rho_L}{2\mu_L}, \tag{10}$$

$$We_0 = \frac{h_0 U_0^2 \rho_L}{2\sigma}, \tag{11}$$

$$Sc_0 = \mu_L / (\rho_L D_L), \tag{12}$$

$$\frac{L_0}{d_{or}} = 4740 Re_0^{-0.8} We_0^{0.07}, \tag{13}$$

$$h_0 = \frac{d_{or}}{\cos(\theta/2)} \left(1 - \sqrt{1 - \frac{4Q\cos(\theta/2)}{U_0 \pi d_{or}^2}} \right), \tag{14}$$

$$U_0 = \sqrt{2\Delta P / \rho_L}, \tag{15}$$

where h_0 is the thickness of sheet, Q is the liquid flow rate and ΔP is pressure loss for nozzle. The physical properties of the nozzle of AA1/12-SS6 are shown in Table 1.

Table 1 Values of L_0 and U_0 (d_{or}=0.003 m)

L_0 ($\times10^{-3}$ m)	Q ($\times10^{-5}$ m^3/s)	U_0 (m/s)	u_{in} (m/s)*
21.9	3.77	5.13	2.5
18.3	4.52	5.73	3.0
15.9	5.15	6.27	3.5

*u_{in} is the initial velocity of the flue gas

The k_{Ld} can be obtained from the results of Brogren and Karlsson (1997) and the penetration time (τ) can be calculated by the diameter distribution of droplets:

$$k_{Ld} = 2\sqrt{\frac{D_L}{\pi\tau}}, \tag{16}$$

$$\tau = \frac{\pi}{4}\sqrt{\frac{\rho_L d^3}{\sigma}}, \tag{17}$$

σ is the liquid surface tension. In the following simulation, Eq.(8) was used to calculate the mass transfer coefficient of the sheet and Eq.(16) was adopted to calculate the mass transfer coefficient of droplets. Because the length of the sheet breakup is short, it is reasonable to assume that U_0 has no change in the sheet and is equal to the initial velocity of the falling droplet.

Moreover, the total area per unit volume at the stage of the sheet can be calculated similar to that of

Yeh and Rochelle (2003). After the sheet turns into droplets, the area per unit volume of the droplets can be calculated by contacting the area per volume (Muginstein *et al*., 2001).

$$a_{\mathrm{Ls}}=\frac{2\pi}{L_0}\left(d_{\mathrm{or}}-2h_0\cos(\theta/2)+L_{\mathrm{b}}\sin(\theta/2)\right), \quad (18)$$

$$a_{\mathrm{Ld}}=6W/(\rho_{\mathrm{L}}\times d), \quad (19)$$

where a is the total area per unit volume, W is the limestone weight concentration in the slurry, d is the particle average diameter. The subscripts 'Ls' and 'Ld' denote the stage of the sheet and the stage of droplets, respectively. The other physical parameters are shown in Table 2.

Table 2 Parameters used in simulations

Parameter	Value
Liquid surface tension σ (N/m)	2.3×10^{-2}
Weight concentration of slurry W (kg/m^3)	0.2
Flue gas density ρ_g (kg/m^3)	1.34
Slurry density ρ_L (kg/m^3)	1200
pH of absorbent ($CaCO_3$ slurry)	5.8
Spray angle θ (°)	70
Temperature T (K)	298

Reactions in the absorption

When upside flow gas contacted the down side limestone spray slurry injected from nozzles, the reaction of both instantaneous equilibrium and the finite rate occurred in the process of absorption. According to the property of the chemical reaction, the hydrolysis of SO_2 and hydrolytic dissociation of HSO_3^- and HCO_3^- can be assumed to be at instantaneous equilibrium through the falling slurry drops (Lancia *et al*., 1997). Therefore, the finite reactions in the absorption are the hydrolysis of CO_2, the oxidation of the calcium sulfite to sulfate, the dissolution on the surface of Calcium carbonate, and the dissolution and crystallization of both sulfite and gypsum.

1. Hydrolysis of CO_2

The rate of the hydrolysis of CO_2 can be written in terms of the gap between the forward and the backward reaction rates:

$$r_{\mathrm{CO_2}}=k_1C_{\mathrm{CO_2}}\left(\frac{C_{\mathrm{H^+}}C_{\mathrm{HCO_3^-}}}{K_{C_1}C_{\mathrm{CO_2}}}-1\right), \quad (20)$$

where r is the rate of the finite reaction and C the molar concentration. The subscripts 'CO_2', 'H^+' and 'HCO_3^-' denote the chemical species. K_{C_1} is the equilibrium constant and k_1 is the rate constant of the forward hydrolysis reaction which can be calculated as the function of temperature according to the results of Pinsent *et al.*(1956).

2. Calcium sulfite oxidation

The rate of sulfite oxidation depends on chemical kinetics, presence of catalysts and mass transfer, and the reaction orders with respect to hydrogen, sulfite and oxygen concentrations (Stromberg, 1992). In this work, the concentration of sulfite was used to calculate the oxidation rate, which can be drawn from Lancia *et al.*(1996):

$$r_{\mathrm{O_2}}=1.95\times10^{10}\mathrm{e}^{-E/(RT)}C_{\mathrm{HSO_3^-}}^{3/2}. \quad (21)$$

3. Limestone dissolution

Assuming the $CaCO_3$ particles have uniform size and are spherical in shape, the equation regarding the dissolution rate of absorbent can be formed by a steady-state mass transfer and the Fick's law of the ions both Ca and C between the limestone surface and the surrounding drops:

$$\frac{1}{b^2}\frac{\partial}{\partial b}(J_kb^2)=r_k, \quad (22)$$

where the subscript 'k' indicates the ions component, S(IV), S(VI), C and Ca. J_k is ion mass flux of the 'k' per square meter, mol/(m^2·s). b is the distance from the center of the limestone particle and r_k is the reaction rate of component k, mol/(m^3·s).

$$\frac{\mathrm{d}C_{\mathrm{Ca^{2+}}}}{\mathrm{d}t}=r_{\mathrm{CaCO_3(di)}}-r_{\mathrm{CaSO_3(c)}}-r_{\mathrm{CaSO_4(c)}}, \quad (23)$$

$$\frac{\mathrm{d}C_{\mathrm{CO_3^{2-}}}}{\mathrm{d}t}=r_{\mathrm{CaCO_3(di)}}-\frac{\mathrm{d}C_{\mathrm{HCO_3^-}}}{\mathrm{d}t}=\frac{\mathrm{d}C_{\mathrm{Ca^{2+}}}}{\mathrm{d}t}. \quad (24)$$

The boundary:

$$b=\infty\Rightarrow[C_k]=[C_k]_{(\mathrm{b})},$$

$$b=\frac{d_{\mathrm{CaCO_3}}}{2}\Rightarrow C_{\mathrm{Ca^{2+}(s)}}=\frac{K_{\mathrm{cp}}}{C_{\mathrm{CO_3^{2-}(s)}}}, \quad (25)$$

where $C_{k(s)}$ is the concentration of component k on the surface of $CaCO_3$, and $C_{k(b)}$ is the concentration of component k in liquid phase (mol/m^3). Subscripts 'di' and 'c' denote the dissolution and crystallization, respectively. K_{cp} is the solubility constant of $CaCO_3$.

The dissolution rate of $CaCO_3$ can be drawn by solving the differential equations proposed by Brogren and Karlsson (1997):

$$r_{\mathrm{CaCO_3\,(di)}} = D_{\mathrm{Ca}}(C_{\mathrm{Ca\,(s)}} - C_{\mathrm{Ca\,(b)}})A_{\mathrm{CaCO_3}}/(0.5d_{\mathrm{CaCO_3}}), \quad (26)$$

where $A_{\mathrm{CaCO_3}}$ is the surface area per volume slurry and D_{Ca} is the diffusive coefficient of the Ca ion (m^2/s).

4. The crystallization and dissolution of $CaSO_3$

Because the reaction tank is sparged with excess of oxygen, the crystallization of calcium sulfite can be assumed to fully occur in falling drops. Based on the effects of H ion in the drops, the crystallization of calcium sulfite is written as (Olausson *et al*., 1993):

$$r_{\mathrm{CaSO_3\,(c)}} = 1.6\times10^{-4}\exp\left(\frac{-5153}{T}\right)\frac{29(RS_{\mathrm{CaSO_3}}-1)^3}{RS_{\mathrm{CaSO_4}}}. \quad (27)$$

(5) The crystallization of gypsum

$r_{\mathrm{CaSO_4\,(c)}}$ is the function of relative saturation of gypsum and can be written as (Brogren and Karlsson, 1997):

$$r_{\mathrm{CaSO_4\,(c)}} = 1.1\times10^{-4}\times3212.6\times(RS_{\mathrm{CaSO_4}}-1). \quad (28)$$

$RS_{\mathrm{CaSO_3}}$ and $RS_{\mathrm{CaSO_4}}$ is the relative saturations which represent the rates of solubility constants divided by the product of the activity of ions:

$$RS_{\mathrm{CaSO_3}} = \frac{C_{\mathrm{Ca^{2+}}}C_{\mathrm{SO_3^{2-}}}}{K_{\mathrm{SP_1}}}, \quad (29)$$

$$RS_{\mathrm{CaSO_4}} = \frac{C_{\mathrm{Ca^{2+}}}C_{\mathrm{SO_4^{2-}}}}{K_{\mathrm{SP_2}}}. \quad (30)$$

Mass balance of elements

The WFGD equipment mainly consists of two segments: the absorber tower and the slurry tank. According to the different chemical reaction equilibrium in each part, the mass balance can be built in the spherical coordinates.

1. The segment of the absorber tower

The material balance for each element is added to the differential equation separately by considering the balance of each ion and charge in the process of falling:

(1) Total mass transfer of S(IV) (SO_2, HSO_3^-, SO_3^{2-}, $CaSO_3$):

$$\frac{\partial C_{\mathrm{S(IV)}}}{\partial t} = \sum_{k=1}^{4}\frac{\nabla(x^2D_k\nabla C_k)}{x^2} - r_{\mathrm{CaSO_3\,(c)}}. \quad (31)$$

The boundary:

$$D_{\mathrm{S(IV)}}\nabla C_{\mathrm{S(IV)},x=R} - \frac{d}{6}\cdot r_{\mathrm{S(IV)},x=R} = 0, \quad (32)$$

where x is distance from gas-liquid interface and R is the radius of droplet.

(2) Total mass transfer of Ca (Ca^{2+}, $CaSO_3$, $CaSO_4$, $CaCO_3$):

$$\frac{\partial C_{\mathrm{Ca}}}{\partial t} = \sum_{k=1}^{4}\frac{\nabla(x^2D_k\nabla C_k)}{x^2} + r_{\mathrm{CaCO_3\,(di)}} - r_{\mathrm{CaSO_3\,(c)}}. \quad (33)$$

The boundary:

$$D_{\mathrm{Ca}}\nabla C_{\mathrm{Ca},\,x=R} - \frac{d}{6}r_{\mathrm{Ca},\,x=R} = 0, \quad (34)$$

(3) The mass transfer of C (CO_3^{2-}, HCO_3^-, H_2CO_3, $CaCO_3$):

$$\frac{\partial C}{\partial t} = \frac{1}{x^2}[\nabla(x^2D_{\mathrm{H_2CO_3}}\nabla C_{\mathrm{H_2CO_3}}) + \nabla(x^2D_{\mathrm{HCO_3^-}}\nabla C_{\mathrm{H_2CO_3^-}}) + \nabla(x^2D_{\mathrm{CO_3^{2-}}}\nabla C_{\mathrm{CO_3^{2-}}})] + r_{\mathrm{CaCO_3\,(di)}}. \quad (35)$$

The boundary:

$$D_{\mathrm{C}}\nabla C_{\mathrm{C},x=R} - \frac{d}{6}r_{\mathrm{C},x=R} = 0. \quad (36)$$

2. The segment of the slurry tank

Based on the overall mass balance of each component (k), the change in concentration can be written as:

$$\frac{\mathrm{d}C_k}{\mathrm{d}t} = N_k + \sum r_k, \tag{37}$$

$$N_k = \frac{1}{V_{\text{tank}}}(Q_{\text{feed}}C_{k,\text{feed}} + Q_{\text{fall}}C_{k,\text{fall}} - Q_{\text{recycle}}C_{k,\text{recycle}} - Q_{\text{discharge}}C_{k,\text{discharge}}), \tag{38}$$

where N is the net accumulation for each element and V is the volume of the tank. The subscripts 'feed', 'fall', 'recycle' and 'discharge' indicate the feed-in slurry, the spray slurry (in absorber), the recycle slurry (in pipe) and the discharged slurry, respectively.

The fresh limestone slurry and oxygen are added to the tank and well-mixed by the agitator. The material balance for each element in the tank is written as:

(1) Total mass transfer of S(VI) (HSO_4^-, SO_4^{2-}):

$$\frac{\mathrm{d}C_{\text{S(VI)}}}{\mathrm{d}t} = N_{\text{S(VI)}} + r_{\text{O}_2} - r_{\text{CaSO}_4\text{(c)}}. \tag{39}$$

(2) Total mass transfer of S(IV) (H_2SO_3, HSO_3^-, SO_3^{2-}, $CaSO_3$):

$$\frac{\mathrm{d}C_{S\text{(IV)}}}{\mathrm{d}t} = N_{S\text{(IV)}} - r_{\text{O}_2} - r_{\text{CaSO}_3\text{(c)}}. \tag{40}$$

(3) Total mass transfer of Ca (Ca^{2+}, $CaSO_3$, $CaSO_4$, $CaCO_3$):

$$\frac{\mathrm{d}C_{\text{Ca}^{2+}}}{\mathrm{d}t} = N_{\text{Ca}^{2+}} + r_{\text{CaCO}_3} - r_{\text{CaSO}_4\text{(c)}} - r_{\text{CaSO}_3\text{(c)}}. \tag{41}$$

(4) The charge balance of total ions in both the absorber tower and the slurry tank:

$$\sum_{k=1}^{n} z_k \frac{1}{b^2}\frac{\partial}{\partial b}(J_k b^2) = 0. \tag{42}$$

The involved ions are H^+, OH^-, HSO_3^-, SO_3^{2-}, HCO_3^-, CO_3^{2-}, HSO_4^-, SO_3^{2-}, Ca^{2+} and z_k is the number of charges of k.

Linking two segments

According to the amount of the transferred species between two segments, the concentrations of the involved elements in each segment are upgraded on the platform of Matlab after every loop.

The different chemical calculations in two segments of the model are illustrated in Fig.1. By adjusting the limestone feed flow rate after each recycle loop, the steady state is achieved when the concentration of the slurry stream entering the absorber is the same as that in the last calculation loop.

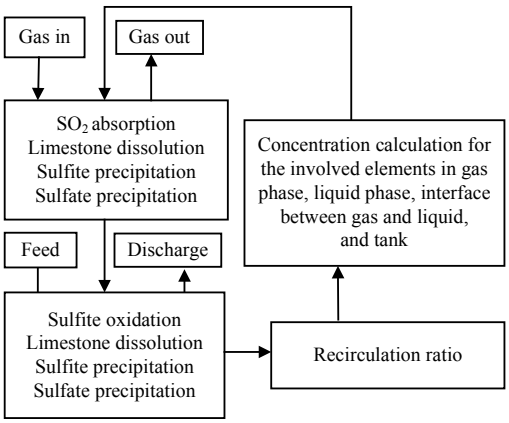

Fig.1 Calculation scheme used in the model

CFD simulations

For better understanding the absorption process, CFD is employed to simulate and exhibit the 3D distribution of the SO_2 concentration in the absorber. In CFD approach, the flue gas is regarded as in continuous phase and the limestone slurry drops are considered to be in discrete phase.

The mass conservation equation for the gas phase and the momentum equation for the ith component are written as:

$$\frac{\partial \rho}{\partial t} + \frac{\partial}{\partial x_i}(\rho \overline{u}_i) = 0, \tag{43}$$

$$\frac{\partial(\rho \overline{u}_i)}{\partial t} + \frac{\partial(\rho \overline{u}_i \overline{u}_j)}{\partial x_j} = -\frac{\partial p}{\partial x_i} + \frac{\partial}{\partial x_j}\left(\mu \frac{\partial \overline{u}_i}{\partial x_j} - \rho \overline{u}_i' \overline{u}_j'\right) + S_{\text{p}}, \tag{44}$$

where S_{p} is the source term conduced by drops in the gas phase in gas-liquid interaction. x_i and x_j are the coordinates (i, j=1, 2, 3).

Turbulence is represented with the (k-ε) model in the continuous phase (i.e., gas in the absorber and slurry in the tank). The correction for turbulence modulation of Lopez de Bertodano (1990) is adopted to account for the effect of the disperse phase.

The mass spices conservation equation is:

$$\frac{\partial \rho}{\partial t}+\frac{\partial(\rho Y_k \bar{u}_i)}{\partial x_i}=\frac{\partial}{\partial x_i}\left(D\frac{\partial(\rho Y_k)}{\partial x_i}\right)+R_k+S_k, \quad (45)$$

where R_k is the net production rate of component (k) by chemical reaction and S_k is the rate of creation by the addition of the dispersed phase with the defined sources.

The above Eqs.(43)~(45) governing differential equations are solved using an iterative solution of the discrete form of the mathematical model. The PC-SIMPLE algorithm is adopted for pressure-velocity coupling with steady integration of the first order implicit formulation and the spatial derivatives by the first order upwind scheme discretization.

Implementation of S_k in fluent via UDF

In the absorber, the total SO_2 absorption rate (J) is equal to the sum of S(IV) fluxes at the gas-liquid interface represented by the mass transfer of both physical absorption and chemical reaction with dissolved limestone. Using a slurry drop as the basic unit to investigate the absorption process, S_k acts as a negative source term in the total flux of SO_2 (mol/(m^2·s)) which can be written as:

$$S_k=-J_{SO_2}=-K_G\alpha(P_{SO_2}-HC_{SO_2}), \quad (46)$$

$$1/K_G=1/k_g+H/(E\times k_L), \quad (47)$$

where K_G is the overall gas mass transfer coefficient (mol/(m^2·Pa·s)) represented by combining k_g (the gas phase mass transfer coefficient, mol/(m^2·Pa·s)) and k_L (the liquid phase mass transfer coefficient).

The enhancement factor (E) can be drawn from the change in the height dependent concentrations along with the height of the absorber by the model calculation in the steady state.

The UDF provided by fluent was employed to write the program, and the effect of the chemical reaction on SO_2 absorption (Eq.(50)) was compiled and loaded on fluent. Based on the two-resistance theory, the absorption of the limestone slurry drops for SO_2 from the gas phase is implemented through calculating the mass transfer process for SO_2 from the continuous phase to the discrete phase.

EXPERIMENTAL APPARATUS

The apparatus consists of a vertical cylindrical absorber, which contains two nozzles and a slurry tank which connects to the limestone feed tank and a discharge pipe. The absorption column was designed so that the gas phase could be sampled from a desired position (two ports were placed with 90° separation in each section). To assure that there was no liquid entering the sample tube, a SO_2 purify washer was installed between the sampling point and the analyzer. The flue gas is made of SO_2 supplied by a high pressure cylinder and N_2 by a liquid-piston rotary compressor which adjusts the SO_2 inlet partial pressures. The absorber is operated counter-currently with the recycled limestone slurry. The feed of limestone slurry and the discharge of the absorber tank were achieved by a pump with flow meter.

The experimental scheme is illustrated in Fig.2.

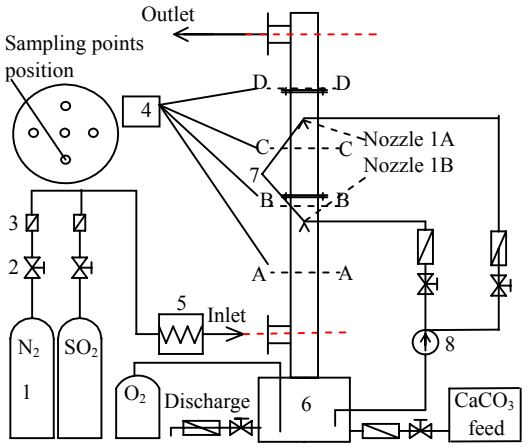

1: air cylinder; 2: control valve; 3: flow meter; 4: SO_2 analyzer
5: mixing and heating; 6: hold tank; 7: spray nozzle; 8: pump

Fig.2 Schematic diagram of experimental apparatus

Experimental investigations were also conducted for various inlet SO_2 partial pressures and velocity to verify the results of CFD. The system was considered to reach a quasi steady state as indicated by no significant changes of output SO_2 concentrations at a stable limestone flow rate and the SO_2 inlet pressure. After that, every sampling point with four times measurements for each one minute interval was carried by RoseMount NGA 2000. Because the experimental system is a column, hybrid tetrahedral grids were used (Fig.3) and the initial condition is given in Table 3.

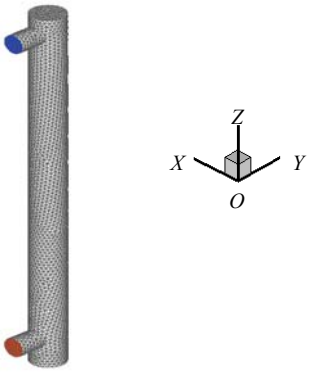

Fig.3 Mesh distribution based on experiment

Table 3 Initial condition for CFD approach

Parameter	Value	Parameter	Value
Height (m)	1	d_{1A} (m) *	0.325
Diameter of scrubber (m)	0.08	d_{1B} (m) *	0.725
Diameter of in/outlet (m)	0.05		

* d_{1A} and d_{1B} are the distances from nozzles 1A and 1B to the outlet of scrubber, respectively

After hitting the wall, the falling drops were regarded as flowing down along the wall, and the calculation of SO_2 source terms in CFD was terminated. Moreover, the BMREQ (Epstein, 1977) is used to calculate the equilibrium constant and solubility product constant.

RESULTS AND DISCUSSION

Enhancement factor of SO_2 absorption

The enhancement factor E is defined as the ratio between the actual absorption rate and the rate which would be observed under the same driving force if no chemical reaction took place (Bird *et al.*, 2002):

$$E=\frac{R_{SO_2}+R_{HSO_3^-}+R_{SO_3^{2-}}}{R_{SO_2}}, \tag{48}$$

$$F=C_{SO_2(i)}-C_{SO_2(b)}, \tag{49}$$

where R is the molar flux of species (mol/(m^2·s)) and F is the driving force of absorption. $C_{SO_2(b)}$ is the SO_2 concentration in liquid phase and $C_{SO_2(i)}$ is the SO_2 concentration on the interface bewteen gas and liquid. Based on the calculation of the model in different cases, the distributions of E as a function of driving force and pH are shown in Fig.4 and Fig.5, respectively.

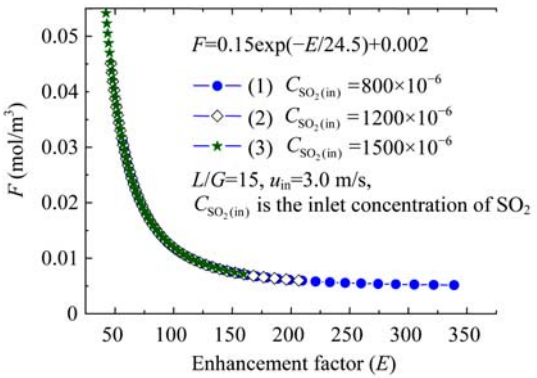

Fig. 4 Relation between E and the driving force

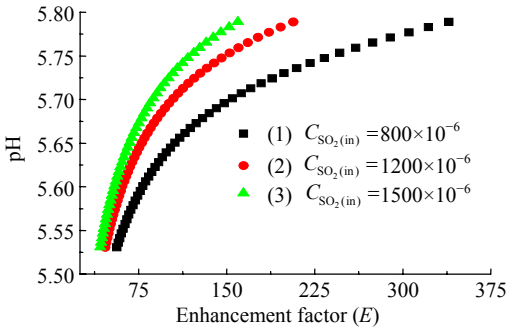

Fig.5 Relation between E and pH

The curves show that E logarithmically decays with increasing value of the driving force (Fig.4) and grows with increasing pH value (Fig.5). It also confirms the past prediction by Lancia *et al.*(1997) which states that E have a value around 50 in the case of a large driving force (0.1 mol/m^3). Moreover, the obtained curves extend the effects of the driving force on enhancement.

Fig.5 shows that the enhancement factor has the highest value close to the nozzle, owing to the low driving force and the high pH value (the fresh alkaline absorbent). It also indicates that the enhancement factor decreases with the increasing inlet SO_2 concentration. It can be explained by the fact that the SO_2 dissolves faster as the concentration of SO_2 on the gas-liquid interface increases, but the limestone dissolution rate does not increase as fast as that of SO_2.

In order to clarify the influences of different variables on SO_2 removal efficiency, 10 cases were performed by both the experimental measurement and

the model calculation; parameters are shown in Table 4 and the results are shown in Figs.6~10.

Table 4 Cases testing for the influence of variables on the SO_2 removal efficiency

Case	$C_{SO_2(in)}$ ($\times10^{-6}$)	u_{in} (m/s)	λ
(a)	800	3	15
(b)	1200	3	15
(c)	1500	3	15
(d)	1200	2.5	15
(e)	1200	3.5	13
(f)	800	3	13
(g)	1200	3	13
(h)	1500	3	13
(i)	1200	3	11
(j)	1500	3.5	15

Regarding to the SO_2 absorption rate, Fig.6 shows that the prediction value of the model is always a little lower than the measurement value of the experiment. It can be attributed to the simplification in the model, in which the calculations for residence time and interfacial area are less than those in the actual experiment.

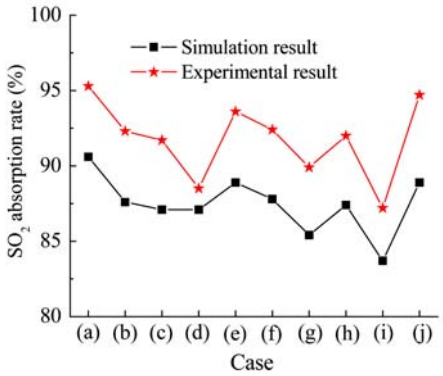

Fig.6 Comparison between model and experimental results for SO_2 absorption rate

However, the differences, which are less than 10% in all cases, demonstrate that the combined model with the enhancement factor reacts correctly to the changes in operating variables and can be used to simulate the process of SO_2 absorption with the falling limestone drops.

The relation between the driving force F and the enhancement factor E can be drawn by curve fitting and be added to the UDF for simulations:

$$F=0.15\exp(-E/24.5)+0.002. \quad (50)$$

Distribution of SO_2 concentration

Initial gas flow rate and SO_2 concentration are 3 m/s and 1200×10^{-6}, respectively, with $CaCO_3$ spray slurry. The SO_2 concentration profile in the Y=0 section and four sections along Z axis (whose positions are shown in Fig.2) are shown in Fig.7. Fig.7 shows that turbulence is formed in the section from the inlet to the downside of the nozzle after the gas flows into the absorber. The SO_2 concentration distributions on Z axis clearly indicate that the volume fraction of gas is significantly reduced along the column height due to the absorption. Moreover, it indicates that the contour of flue gas spirally moves to the outlet.

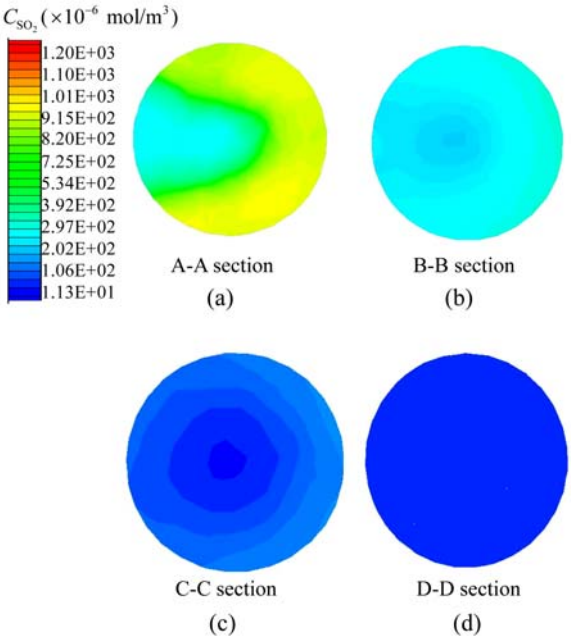

Fig.7 SO_2 concentration profile in process of absorption. (a) Z=0.225 m; (b) Z=0.425 m; (c) Z=0.625 m; (d) Z=0.825 m

For clearly describing the distribution of SO_2 in the process of absorption, data from four sections were collected from CFD and experimental measurement. The SO_2 distribution in the direction of X axis was plotted in Fig.8. Fig.8 shows that the distribution of SO_2 along X axis is unsymmetrical. Firstly, the right wall modifies the momentum transfer between gas and spray droplets. Secondly, its influence is to reject the droplets back into the continuous phase flow after their interaction with the wall. Furthermore, it can be further justified by the drag force near the

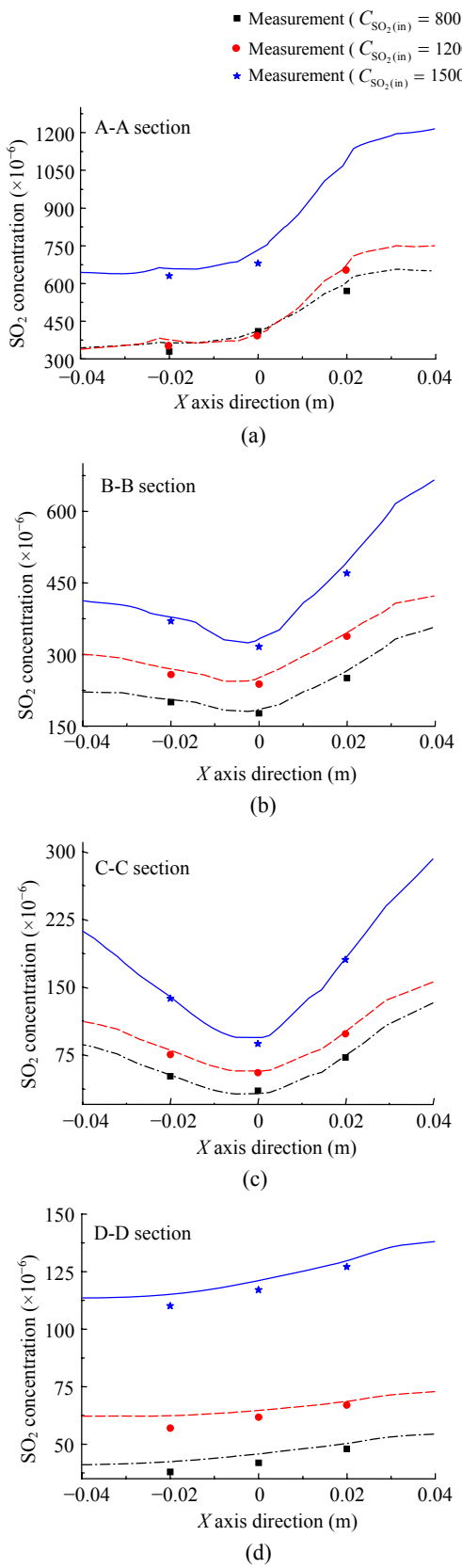

Fig.8 SO_2 distribution in the direction of *X* axis (a) *Z*= 0.225 m, (b) *Z*=0.425 m, (c) *Z*=0.625 m, (d) *Z*=0.825 m

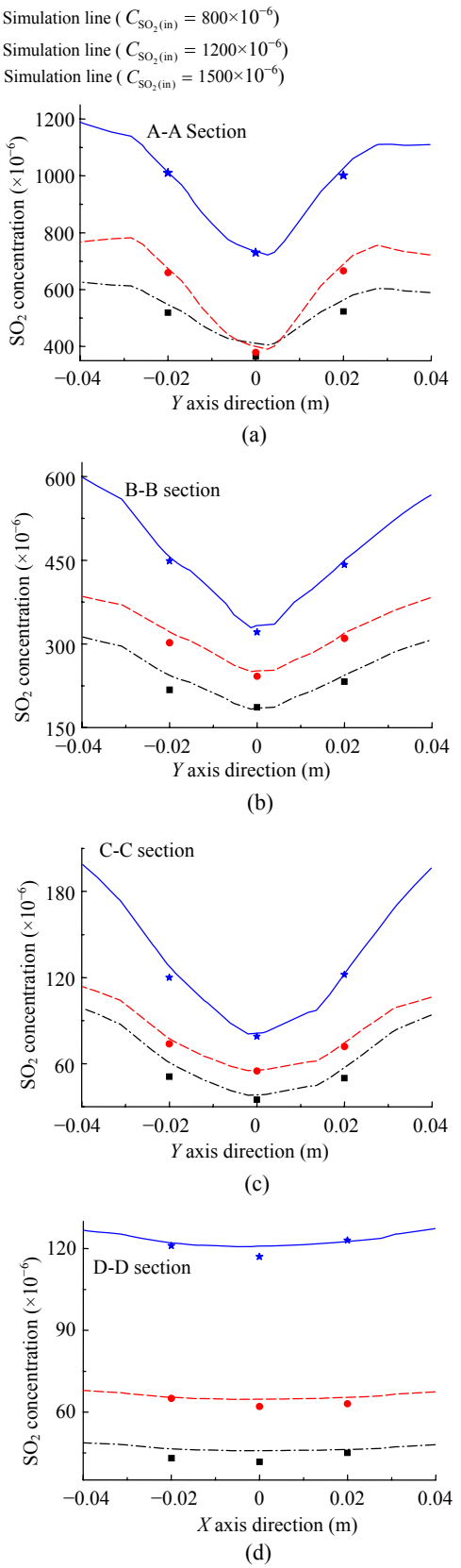

Fig.9 SO_2 distribution in the direction of Y axis. (a) *Z*= 0.225 m, (b) *Z*=0.425 m, (c) *Z*=0.625 m, (d) *Z*=0.825 m

wall which can be 20%~30% larger (Han *et al*., 1991) which produces the reduction in droplet residence time and subsequently increases the SO_2 concentration around the area of wall.

The SO_2 distribution in the direction of Y axis is plotted in Fig.9. Unlike the situation observed in the concentration field along X axis, there is a reflectional symmetry concentration shift (along with Y=0). The concentration contours are parallel to the streamlines, and the lowest SO_2 concentration is attained at the vortex center where the turbulence density is the highest. This indicates that the strong reduction in the gas volume fraction lowers the momentum transfer of the drops and that the flow structure is changed. Furthermore, faster reaction kinetics (higher turbulence density) evidently leads to a faster consumption of SO_2, leading to a lower value in the SO_2 profile.

Influences of operating variables

The SO_2 removal efficiency (η) is defined as

$$\eta = (C_{SO_2(in)} - C_{SO_2(out)}) / C_{SO_2(in)}, \quad (51)$$

where the subscripts 'in' and 'out' denote the inlet and outlet of scrubber, respectively.

1. The effect of inlet SO_2 concentration on η

The influence of inlet SO_2 concentration on efficiency was shown in Figs.10a~10c. An increase in inlet concentration from 800×10^{-6} to 1500×10^{-6} causes a decrease of η from 90.6% to 87.1%, respectively. As the SO_2 concentration (partial pressure) at the inlet increases, the mass transfer of SO_2 into the droplet increases, which contributes to an increase in the concentration of HSO_3^- in the drops and subsequently hinders the absorption of SO_2.

2. The influence of inlet flow rate on η

Keeping the other parameters constant, the simulations were carried with different flow rates and the results were reported in Figs.10d, 10e, 10f and 10h which indicates that η increases with the growing flow rate. It can be explained by the fact that the increased flue gas velocity enhanced the SO_2 momentum and subsequently increased the total gas hold-up (Romain *et al*., 2008). The enhancing influence of limestone particles on the absorption of SO_2 depends on the duration of the exposure time of the liquid surface to the gas.

Moreover, a higher velocity increases the turbulence in the gas phase and, even more importantly, increases the slurry hold-up (amount of drops in a defined volume) in the absorber (Vandu *et al*., 2005). Longer exposure duration would lead to larger enhancement effect of the solid particles and subsequently increase the SO_2 removal efficiency.

3. The influence of the rate of L/G (λ) on η

Keeping the inlet flue rate as 3 m/s and the SO_2 concentration as 1200×10^{-6} mol/m^3, the SO_2 contours in different λ values are drawn by simulation shown in Figs.10b, 10g, 10i.

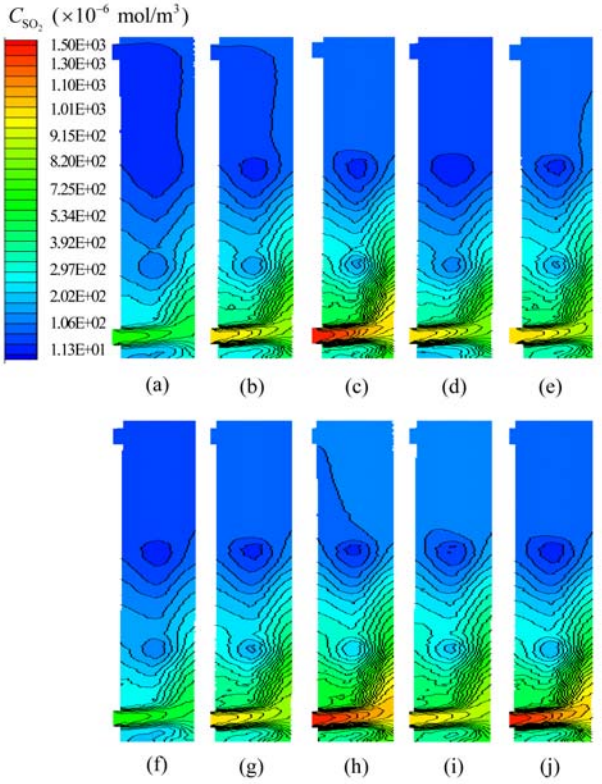

Fig.10 Cases (a)~(j) simulating SO_2 absorption for different parameters

The results indicate that η is 87.6%, 85.4% and 83.7% respectively at the λ value of 15, 13, and 11. It can be explained that the increase in spray amount enhances the interfacial areas for mass transfer between the SO_2 and the limestone absorbent. Therefore, λ is an important parameter for achieving satisfactory SO_2 removal efficiency with consideration of the operating cost.

CONCLUSION

In order to better understand the effects of spray on SO_2 absorption in WFGD, a model incorporating the continuous changes in pH has been presented. The relationship between the enhancement factor and pH value as well as the driving force has been explored. The model shows that the enhancement factor grows with increasing pH values and logarithmically decays with increasing driving force values. A comparison of the SO_2 concentration between the experiments and the calculations indicate that this model can be used to offer a more cost-effective and timely prediction for the SO_2 absorption process. Moreover, the influence of important operating variables was determined and the results can be used to provide designers with more confidence in system optimization.

References

Akbar, M.K., Yan, J., Ghiaasiaan, S.M., 2003. Mechanism of gas absorption enhancement in a slurry droplet containing reactive, sparingly soluble micro particles. *International Journal of Heat and Mass Transfer*, **46**(24):4561-4571. [doi:10.1016/S0017-9310(03)00296-5]

Alexandrova, S., Marion, M., Lepinasse, E., Saboni, A., 2004. Mass transfer modeling of SO_2 into large drops. *Chemical Engineering & Technology*, **27**(6):676-680. [doi:10.1002/ceat.200401655]

Altwicker, E.R., Lindhjem, C.E., 1988. Absorption of gases into drops. *AIChE Journal*, **34**(2):329-332. [doi:10.1002/aic.690340218]

Amokrane, H., Caussade, B., 1999. Gas absorption into a moving spherical water drop. *Journal of the Atmospheric Sciences*, **56**(12):1808-1829. [doi:10.1175/1520-0469(1999)056<1808:GAIAMS>2.0.CO;2]

Bausach, M., Pera, T.M., Fite, C., 2006. Water-induced rearrangement of $Ca(OH)_2$ reacted with SO_2. *AIChE Journal*, **52**(8):2876-2886. [doi:10.1002/aic.10907]

Bird, R.B., Stewart, W.E., Lightfoot, E.N., 2002 Transport Phenomena (2nd Edition). Wiley, New York.

Brogren, C., Karlsson, H.T., 1997. Modeling the absorption of SO_2 in a spray scrubber using the penetration theory. *Chemical Engineering Science*, **52**(18):3085-3099. [doi:10.1016/S0009-2509(97)00126-7]

Ebrahimi, S., Kleerebezem, R., Loosdrecht, M.C., Heijnen, J.J., 2003. Kinetics of the reactive absorption of hydrogen sulfide into aqueous ferric sulfate solutions. *Chemical Engineering Science*, **58**(2):417-427. [doi:10.1016/S0009-2509(02)00522-5]

Epstein, M., 1977. EPA Alkali Scrubbing Test Facility: Summary of Testing Through October 1974. U.S. EPA 600/7-7-105.

Gerbec, M., Stergarsek A., Kocjancic R., 1995. Simulation model of wet flue gas desulphurization plant. *Computers and Chemical Engineering*, **19**(1):283-286. [doi:10.1016/0098-1354(95)87050-4]

Gomez, A., Fueyo, N., Tomas, A., 2007. Detailed modeling of a flue-gas desulfurisation plant. *Computers and Chemical Engineering*, **31**(11):1419-1431. [doi:10.1016/j.compchemeng.2006.12.004]

Haider, A., Levenspiel, O., 1989. Drag coefficient and terminal velocity of spherical and nonspherical particles. *Powder Technology*, **58**(1):63-70. [doi:10.1016/0032-5910(89)80008-7]

Han, K.S., Chung, M.K., Sung, H.J., 1991. Application of Lumley's drag reduction model to two-phase gas-particles flow in pipe. *Journal of Fluids Engineering*, **113**(1):130-136. [doi:10.1115/1.2926485]

Hikita, H., Asia, S., Takatsuka, T., 1972. Gas absorption with a two step instantaneous chemical reaction. *The Chemical Engineering Journal*, **4**(1):31-40. [doi:10.1016/0300-9467(72)80050-9]

Kadja, M., Bergeles, G., 2003. Modeling of slurry droplet drying. *Applied Thermal Engineering*, **23**(7):829-844. [doi:10.1016/S1359-4311(03)00014-0]

Kota, K., Langrish, T.A.G., 2007. Prediction of wall deposition behavior in a pilot-scale spray dryer using deposition correlations for pipe flows. *Journal of Zhejiang University SCIENCE A*, **8**(2):301-312. [doi:10.1631/jzus.2007.A0301]

Lancia, A., Musmarra, D., Pepe, F., Volpicelli, G., 1994. SO_2 absorption in a bubbling reactor using limestone suspensions. *Chemical Engineering Science*, **49**(24):4523-4532. [doi:10.1016/S0009-2509(05)80242-8]

Lancia, A., Musmarra, D., Pepe, F., 1996. Uncatalyzed heterogeneous oxidation of calcium bisulfite. *Chemical Engineering Science*, **51**(16):3889-3896. [doi:10.1016/0009-2509(96)00222-9]

Lancia, A., Musmarra, D., Pepe, F., 1997. Modeling of SO_2 absorption into limestone suspensions. *Industrial & Engineering Chemistry Research*, **36**(1):197-203. [doi:10.1021/ie9602365]

Lopez de Bertodano, M., Lee, S.J., Lahey, R.T., Drew, D.A., 1990. The prediction of 2-phase turbulence and phase distribution phenomena using a Reynolds stress model. *Journal of Fluids Engineering*, **112**(1):107-114. [doi:10.1115/1.2909357]

Muginstein, A., Fichman, M., Gutfinger, C., 2001. Gas absorption in a moving drop containing suspended solids. *International Journal of Multiphase Flow*, **27**(6):1079-1094. [doi:10.1016/S0301-9322(00)00063-X]

Nagel, D., Richard, K.D., Lintnz, H.G., Roizard, C., Lapicque, F., 2002. Absorption of sulfur dioxide in *N*-formylmorpholine: investigations of the kinetics of the liquid phase reaction. *Chemical Engineering Science*, **57**(22):4883-4893. [doi:10.1016/S0009-2509(02)00283-X]

Olausson, S., Wallin, M., Bjerle, I., 1993. A model for absorption of sulphur dioxide into a limestone slurry. *The Chemical Engineering Journal*, **51**(2):99-108. [doi:10.1016/0300-9467(93)80016-H]

Pinsent, B.R.W., Pearson, L., Roughton, F.J.W., 1956. The

kinetics of the combination of carbondioxide with hydroxide ions. *Transactions of the Faraday Society*, **52**(1): 1512-1522. [doi:10.1039/TF9565201512]

Retieb, S., Guiraud, P., Angelov, G., Gourdon, C., 2007. Hold-up within two-phase countercurrent pulsed columns via Eulerian simulations. *Chemical Engineering Science*, **62**(17):4558-4572. [doi:10.1016/j.ces. 2007.04. 043]

Romain, L., Arsam, B., Laurent, S., Yannick, J.H., Rachid, O., Badie, I.M., 2008. An algorithm for predicting the hydrodynamic and mass transfer parameters in bubble column and slurry bubble column reactors. *Fuel Processing Technology*, **89**(1):322-343. [doi:10.1016/j.fuproc. 2007.11.016]

Saboni, A., Alexandrova, S., 2001. Sulfur dioxide absorption and desorption by water drops. *Chemical Engineering Journal*, **84**(3):577-580. [doi:10.1016/S1385-8947(01) 00172-3]

Scala, F., D′Ascenzo, M., Lancia, A., 2004. Modeling flue gas desulfurization by spray-dry absorption. *Separation and Purification Technology*, **3**4(1-3):143-153. [doi:10.1016/ S1383-5866(03)00188-6]

Sheng, Y.L., Wen, D.X., 2006. Modeling and simulation of a bubbling SO_2 absorber with granular limestone slurry and an organic acid additive. *Chemical Engineering & Technology*, **29**(10):1167-1173. [doi:10.1002/ceat.2006 00101]

Stromberg, A.M., 1992. Prospects for Further Development of Spray-scrubbing. PhD Thesis, University of Lund.

Vandu, C.O., Berg, B.V.D., Krishna, R., 2005. Gas-liquid mass transfer in a slurry bubble column at high slurry concentrations and high gas velocities. *Chemical Engineering & Technology*, **28**(9):998-1002. [doi:10.1002/ceat.200500 151]

Yeh, N.K., Rochelle, G.T., 2003. Liquid-phase mass transfer in spray contactors. *AIChE Journal*, **49**(9):2363-2373. [doi:10.1002/aic.690490912]

Zhang, Q.Y., Wei, Y.M., Chen, Y.X., Guo, H., 2007. Environmental damage costs from fossil electricity generation in China, 2000-2003. *Journal of Zhejiang University SCIENCE A*, **8**(11):1816-1825. [doi:10.1631/jzus.2007. A1816]